

## Study of form and structure in an injection molding process for polyethylene/polycarbonate and polyethylene/polyethylene terephthalate blended parts

Hesamedin Habibi<sup>1a</sup>, Siamak Hosseinzadeh<sup>2b</sup>, Ramin Ghasemiasl<sup>3c</sup>, Meghdad Rahimi Galogahi<sup>4d</sup>

<sup>1</sup>Department of Mechanical Engineering, University College of Rouzbahan, Sari, Iran

<sup>2,3</sup>Department of Mechanical Engineering, West Tehran Branch, Islamic Azad University, Tehran, Iran

<sup>4</sup>Department of Mechanical Engineering, Islamic Azad University, Behshahr Branch, Mazandaran, Iran

Received: March 19, 2015

Accepted: May 2, 2015

### ABSTRACT

The skin-core structure of injection molded poly(ethylene terephthalate) (PET)/polyethylene (PE) and polycarbonate (PC)/PE blends was investigated. The morphology and microstructure in an injection molding for polyethylene/polyethylene terephthalate and polyethylene/polycarbonate blended parts were investigated by SEM images. The hollow cube part produced two levels of injection as speed processing parameter. The morphology in the section perpendicular to the melt flow direction included four layers, surface, sub-skin, intermediate layers as well as core zone. The surface layer was ignored in the present study. The immiscible PET and PC particles were scattered into matrix PE. The skin layer was ignored in this research. The results indicate that the scattered particles in the sub skin layer are elongated and fibrous. The scattered particles in the core zone were spherical and the intermediate layer exists between these two layers. The scattered particles in this layer were ellipsoidal. In this research, the impact of injection speed parameter on microstructure was explored. Furthermore, morphological exploration was performed and the diameter of the scattered particles was examined in the three layers, by comparing a cross section of the specimen. The results indicate that the size, shape and microstructure properties depended not only on the type and material properties, but also on the injection parameters such as injection speed and the positions in the molded parts.

**KEYWORDS:** Injection Molding, Mold Flow, Molding Analysis, Microstructure and SEM Picture, Injection Molding.

### 1. INTRODUCTION

The plastic injection molding process is known as an approach for mass production, and it is performed by the injection machines and molds. In this process, on one hand, mold and injection machine parameters affect the molding process. The mold and machine parameters include part geometry, type and injection gate geometry (the place where molten material enters the mold, type and runner geometry, material type, molten material temperature, mold body temperature, injection pressure, injection speed, cooling approach, cooling time, shrinkage percent and etc and, on the other hand, the molding process are hardened by the nature of the plastic material properties [1-4].

Many production parts are the blends of the several polymers (plastic, rubber...). The polymer blended parts experienced two processing melting temperatures. One of them is the temperature that polymer blends are made and, the other is the temperature that polymer blended parts are made; both of this temperature play an important role in the final structure of the parts [5, 6]. Several parameters affected the type and size of the scattered phase in the matrix phase, morphology type, mixing time, shear stress and viscosity ratio during the production. The effects of these parameters investigated in some researches [7, 8]. Plastic injection molding process is known as one of the most important and applicable approaches to produce polymer blended parts. [5,6]. Karger-kocsis and Scikal [6] explored relation between structure properties such as the failure phenomenon of injection molded polypropylene (PP) blends modified with ethylene/propylene/dieneterpolymer and thermoplastic polyolefinic rubber with processing parameters. It was found that skin-core morphology was formed in both the pure PP matrix as well as the modified PP blends with rubber particles of various deformations in injection molding process.

Karger-kocsis and Mouzakis [9] investigated skin-core structure in the systems containing Rubber-Toughened Polypropylene (RTPP) in the failure in the injection molding process.

RTPP with the high percent of the rubber particles witnessed no skin-core morphology in the PP matrix structure: in contrast, RTPP with the low percent of the rubber scattered particles formed the skin-core structure. particles.

Fellahi et al. [10, 11] have studied the morphological behaviors of injection molded HDPE/PA6 blends with and without a Compatibilizer. They have investigated and found in the sub-skin layer that the scattered phase in the matrix phase of blended part has oriented with flow direction increasingly.

Karger-kocsis and Fellahi et al. have showed by Scanning electron microscope (SEM) that a thin surface layer of parts have only contained matrix phase, and morphological behavior from surface layer to core layer have contained the

scattered phase in the matrix phase. The precise analyses performed have revealed that both the matrix phase and scattered phase in surface layers of parts have contained the same composition of the interior layers of the parts.

Son [12] studied the viscosity rate influence, injection molding condition and Compatibilizer on the injection molded polyphenylene oxide/PA6 blended part structure. In this research, regarding the low viscosity rates, discrete layers: surface, sub-skin and core layers was found, but for high viscosity rates, beside these layers, another interior layer was found with low deformation in the scattered phase. This layer was named intermediate layer, and it was formed between surface layer and core layer

Generally, there are few studies on the blend systems especially on comparing on the injection molded blends with different properties together as well as the relationship between morphology and mechanical properties [6-14]. Therefore, great efforts are needed to fully understand the injection molded part morphologies. In this research, the microstructures and morphological behaviors of the injection parts for two immiscible polymer blends are investigated. The first polymer blend contains polyethylene terephthalate (PET)/polyethylene (PE) and the second polymer blend include polycarbonate (PC)/polyethylene. The reason for this material selection is that PE/PET blend is a typical semi crystalline/semi crystalline system with a viscosity ratio less than one, and PE/PC blend is a typical semi crystalline/amorphous system with a viscosity ratio higher than one.

## 2. Materials and Methods

The plastic materials used in this research were High density polyethylene (HDPE), Poly ethylene terephthalate (PET) and Polycarbonate (PC). These materials were supplied from Iranian companies including the Golpaygan Petrochemical company.

The studied part is a hollow cube with a length of 160 mm, width of 80 mm and height of 20 mm. The thickness in the wall is 3 mm, and is 4 mm in the bottom. The vertical edges in the part were filleted in four different radii; Figure 1 shows the part. This part was injected from the smaller side edge, and the injection gate (fan gate type) was chosen 40 mm long and 1.5 mm deep. For this part, a mold was designed and manufactured. Figure 2 shows the manufactured mold with injection part.

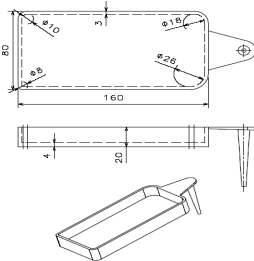


**Figure .1.** The dimensions of the injection part and gate



**Figure.2.** The manufactured mold and injection part.

## 3. Molding process

The plastic materials used in this research were dried before the molding process for at least 10 h, to avoid hydrolytic degradation at 90°C. Both PE/PET and PE/PC blends were mixed together at a weight ratio of 75/25, and were dried simultaneously. The mixtures were blended in a twin-screw extruder at a screw speed of 90 rpm and heating profile from 180 to 265°C from hopper to nozzle. The parts were molded using a 125/380 injection molding machine made in Poolad Company, Iran. The heating profile was 220 to 265°C from hopper to injection nozzle. The injection molding process was repeated several times for the selected polymer blends to achieve stable conditions. On the other hand, these repetitions resulted in the release of materials remaining from former molding processes. Figure 3 shows the mounted mold on the injection machine, and the stable molding conditions are shown for two low and high injection speeds (Table 1). In this research, all adjustable parameters were assumed constant under molding conditions, only the injection speed was varied in the two levels.



**Figure.3.** the mounted mold on the injection machine

Table 1. molding conditions

|        | Inj. pre (MPa) | Packing Pre (MPa) | M. Tem (C) | Cooling Time (s) | Inj. cycle Time(s) | Inj. Time (s) | Inj. Speed (%) |
|--------|----------------|-------------------|------------|------------------|--------------------|---------------|----------------|
| Level1 | 77             | 70                | 22         | 15               | 35                 | 7.5           | 15             |
| Level2 | 77             | 70                | 22         | 15               | 35                 | 2.5           | 77             |

The tensile test specimens were cut at the base of the ASTM D638. Figure 4 shows a test specimen that was cut from the bottom of the part.



**Figure. 4.**a schematic test specimen that was cut from the bottom of the part.

**Figure. 5.**shows a test specimen that was cut from the bottom of the part

**4. Morphological observations**

The morphological images were prepared using a scanning electron microscope (SEM) from Razi Metallurgy Institute, Iran. The test specimens were frozen in liquid nitrogen for one hour, then the impact was broken to make surfaces for observation. One of these fracture sections is close to the injection gate, while the other is far from the injection gate. These sections are named (A-A) and (B-B) sections. These sections are shown in Figure 6.

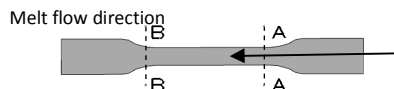


**Figure.6.**(A-A) section; near to the injection gate and (B-B) section; far from the injection gate.

**5. Results and Discussion**

Figure 7 illustrates samples of micrographs for PE/PET and PE/PC blends. In this research, the skin-core distribution was used in agreement with some earlier researches [6-12]. The failure section was divided into the skin, sub-skin, intermediate and core layers, based on such distribution. The degree of deformation increased in the surface layers, in contrast to the interior layers. In this research, the skin layer was ignored. Figure 7 shows that the PET and PC particles in the PE matrix, appeared in the spherical and ellipsoidal form.

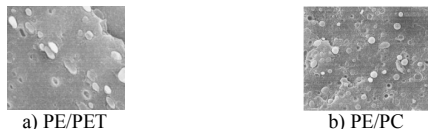


**Figure.7.** illustrates samples of micrograph for PE/PET and PE/PC blends

On the other hand, the shrinkage percent of the PE parts is more than the PET and PC parts [1], and, as a result, no detachment and coalescence exists in the boundary between the scattered and matrix phases. The minimum, maximum and average diameters of the PET and PC particles in SEM images of Figure 7 are examined and summarized in Table 2.

Table 2. minimum, maximum and average diameters of the PET and PC particles in SEM image of figure 7

|             | Min and maxdia | avedia |
|-------------|----------------|--------|
| PE/PET (μm) | 0.3-3.2        | 1.1    |
| PE/PC (μm)  | 0.15-1.4       | 0.8    |

Figures 8 to 15 show SEM images in two near and far sections of the injection gate for every part at two levels of injection speeds in three layers of cross sections namely 1) sub-skin, 2) intermediate and 3) core layers.

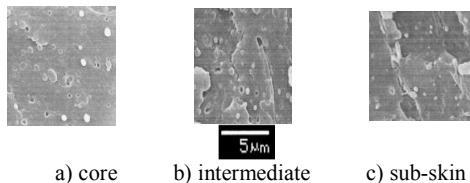


**Figure.8.** SEM images: a) core, b) intermediate and c) sub-skin layers for (A-A) section in low injection speed for the PE/PET blend.

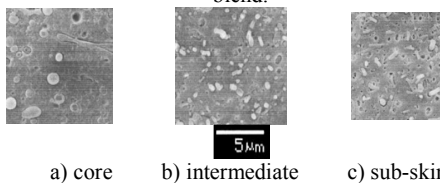


**Figure. 9.** SEM images: a) core, b) intermediate and c) sub-skin layers for (A-A) section in low injection speed for the PE/PC blend.

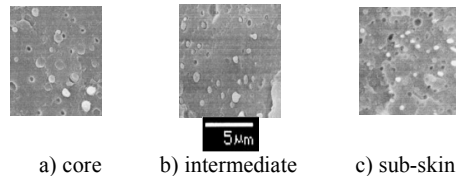


**Figure. 10.** SEM images: a) core, b) intermediate and c) sub-skin layers for (A-A) section in high injection speed for PE/PET blend.

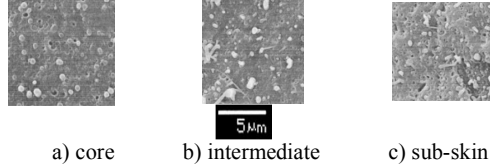


**Figure.11.** SEM images: a) core, b) intermediate and c) sub-skin layers for the (A-A) section in high injection speed for the PE/PC blend.

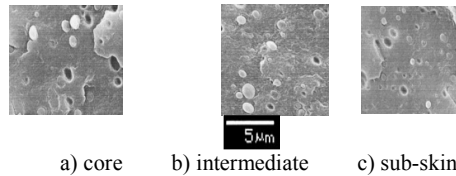


**Figure.12.** SEM images: a) core, b) intermediate and c) sub-skin layers for (B-B) section in low injection speed for the PE/PET blend.

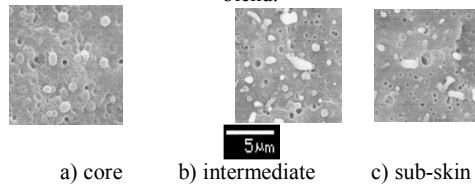


**Figure.13.** SEM images: a) core, b) intermediate and c) sub-skin layers for (B-B) section in low injection speed for the PE/PC blend.

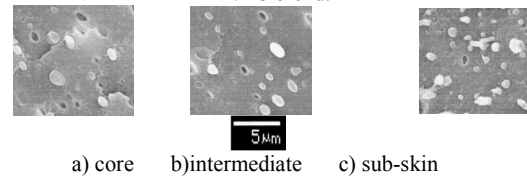


**Figure.14.** SEM images: a) core, b) intermediate and c) sub-skin layers for the (B-B) section in high injection speed for the PE/PET blend.

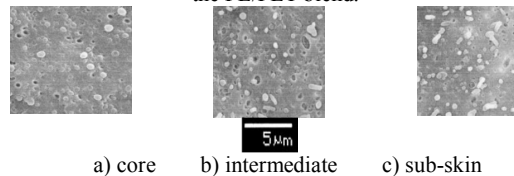


**Figure.15.** SEM pictures: a) core, b) intermediate and c) sub-skin layers for the (B-B) section in high injection speed for the PE/PC blend

In Figures 8 to 15, the spherical, ellipsoidal and elongated particles in the SEM images are PET and PC particles, scattered in the PE matrix. The microstructure of the cross-sections perpendicular to the flow direction had four layers namely 1) surface, 2) sub-skin, 3) intermediate and 4) core layers. Ignoring the surface layer, the sub-skin layer was included among the elongated fiber particles. The core included the spherical particles scattered in the PE matrix, and between these two layers exist the intermediate layer which includes ellipsoidal particles, and in this layer, spherical and elongated particles were also seen. Tests were performed at two low and high injection speeds. At the low injection speed, the PET particles scattered in the PE matrix were spherical and ellipsoidal, but at the high injection speed, these particles showed more trends to elongation in the sub-skin layer. In contrast, at both levels of injection speed, PC particles

scattered in the PE matrix were more elongated than the PET particles. The minimum, maximum and average diameters of the PET and PC particles in the SEM images of Figures 8 and 15 were examined and summarized in Tables 3 and 4.

Table 3. minimum, maximum and average diameters of the PET particles in SEM images of Figures 8 to 15

| PE/PET | Failure sections and injection speed levels | Layers in sections in thickness direction |              |                      |              |                      |              |
|--------|---|---|--------------|----------------------|--------------|----------------------|--------------|
|        |   | Sub- skin                                 |              | Intermediate         |              | Core                 |              |
|        |   | min and max dia (µm)                      | ave dia (µm) | min and max dia (µm) | Ave dia (µm) | min and max dia (µm) | Ave dia (µm) |
| (A-A)  | Low   | 0.2-0.9                                   | 0.7          | 0.2-1.5              | 0.9          | 0.3-3                | 1            |
|        | High  | 0.2-0.9                                   | 0.5          | 0.2-1.3              | 0.7          | 0.2-1.9              | 0.9          |
| (B-B)  | Low   | 0.3-2.2                                   | 1.6          | 0.4-2.7              | 1.6          | 0.2-3.3              | 1.8          |
|        | High  | 0.4-1.6                                   | 0.6          | 0.2-1.9              | 1.1          | 0.3-3                | 1.6          |

Table 4. minimum, maximum and average diameters of PC particles in SEM images of Figures 8 to 15

| PE/PET | Failure sections and injection speed levels | Layers in sections in thickness direction |              |                     |              |                     |              |
|--------|---|---|--------------|---------------------|--------------|---------------------|--------------|
|        |   | Sub- skin                                 |              | Intermediate        |              | Cora                |              |
|        |   | Min and max dia(µm)                       | Ave dia (µm) | min and maxdia (µm) | Ave dia (µm) | min and maxdi a(µm) | aved ia (µm) |
| (A-A)  | Low   | 0.2-0.9                                   | 0.5          | 0.3-1.1             | 0.5          | 0.5-2.2             | 1            |
|        | High  | 0.1-1.1                                   | 0.4          | 0.2-1.1             | 0.6          | 0.2-1.2             | 0.7          |
| (B-B)  | Low   | 0.2-1.7                                   | 0.8          | 0.5-0.9             | 0.8          | 0.6-2.4             | 1.3          |
|        | High  | 0.2-1.4                                   | 0.5          | 0.4-1.3             | 0.6          | 0.2-1.6             | 0.8          |

Tables 3, and 4, as well as Figures 8 to 15 show that the diameter of the PET and PC particles in the PE matrix of the (B-B) section, is greater than the (A-A) section in the three layers of the thickness part (sub-skin, intermediate and core layers). On the other hand, the diameter of particles at points far away from the injection gate is more compared to points that are close. As a result, the deformation in the far points of the injection gate is more. Even though, the average diameters of the scattered PET particles at sections far away from the injection gate are more, another additive direction was seen in the particle diameter in every section from the outer to the inner layers. Conversely, the variation range of the particle diameter at points far from the injection gate is more compared to points that are near.. This fact resulted in deformation at points farther from the injection gate, which is more unsystematic. These results and earlier stated additive directions were seen in the scattered PC particles of the PE matrix. Although, the diameter of the scattered PET particle in the PE matrix is increasingly more than the PC particle diameter.

The diameter of the scattered PET and PC particles increased from the surface layer to the core layer. Particles in the core layer appeared to be of spherical shape, and when moved from the core layer to the surface layer, scattered particles became deformed from a spherical to an ellipsoidal shape in the intermediate layer and elongated particle in the sub-skin layer.

**6. Conclusions**

The molding process of the polyethylene/polyethylene terephthalate and polyethylene/polycarbonate blended parts were investigated. The cross-section of the parts based on the degree of particle scattering was divided into four layers namely 1) surface, 2) sub-skin, 3) intermediate and 4) core layers. In this research, the surface layer was ignored. The results are as follows:

1-The diameter of the scattered PET particles, in the PE matrix, is more compared to the PC particles.

2-The microstructure of the section perpendicular to the flow direction includes four layers namely surface, sub-skin, intermediate, and core layers. Having ignored the surface layer, the sub-skin layer included the elongated-fibrous particles. The core layer included the spherical particles scattered in the PE matrix. Between these layers exists the intermediate layer that included the ellipsoidal particles and also a few elongated and spherical particles.

3-The average diameter of the scattered particles in the matrix phase at points close to the injection gate is smaller compared to points far away.

4-The average diameter of the scattered particles in the matrix phase at the low injection speed is more than at the high injection speed, in the three studied layers of the part thickness.

5-The shape, size and properties of the microstructure of the scattered PET and PC particles in the matrix phase depend not only on material properties, but also on the injection parameters such as injection speed and the different studied cross-sections of the part.

## REFERENCES

1. J. M. Fischer, Handbook of molded part shrinkage and warpage, Published USA by Plastic Design Library/W. Andrew. Inc, 13 Eaton Avenues, Norwich, New York 13815, 2003.
2. G. Menges, W. Michaeli, P. Mohren, How to make injection molds, Third Edition, Hanser Publishers, Munich, 2001.
3. J. Shomakers, Moldflow design guide, Hanser Publishers. Framingham, Massachusetts, USA, 2006.
4. S. Thompson, Handbook of mold, tool and die repair welding, Abington Publisher, Abington, Cambridge CB1 6AH, England, 1999.
5. J. R. A. Pearson, Mechanics of polymer processing, Elsevier Applied Science, London, 1998.
6. K. Kocsis, I. Csikai, Skin-core morphology and failure of injection molded specimens of impact-modified polypropylene blends. *Polymer*, pp. 27-41. 1987.
7. H. Ahmadi, G. Liaghat, M. MehrdadShokrieh, Experimental investigation of fabrication parameter's effects on the mechanical properties of epoxy/ceramic microballoon syntactic foam, *Modares Mechanical Engineering*, Vol. 14, No. 2, pp. 47-54, 2014. (In Persian)
8. M. MehrdadShokrieh, M. Elahi, A new model to estimate the Young's modulus of polymer concrete using micromechanical relations, *Modares Mechanical Engineering*, Vol. 12, No. 2, pp. 153-162, 2012. (In Persian)
9. K. Kocsis and D. E. Mouzakis, Effects of injection molding-induced morphology on the work of fracture parameters in rubber-toughened polypropylenes, *Polymer Engineering Science*, pp. 39-65, 1999.
10. S. Fellahi, B. D. Favis and B. Fisa, A modified model predictions and experimental results of weld-line strength in injection molded PS/PMMA blends, *Polymer*, pp. 37-46, 1996.
11. S. Fellahi, B. D. Favis and B. Fisa, Tensile dilatometry of injection-moulded HDPE/PA6 blends, *SPE ANTEC Tech, Pap*, 1993.
12. Y. Son, K. H. Ahn and K. Char, Morphology of injection molded modified poly(phenylene oxide)/polyamide-6 blends, *Polymer Engineering Science*, pp. 40-52, 2000.
13. B. D. Favis, *Polymer Blends Vol. 1: Formulation*, edited by D. R. PAUL, and C. D. Bunall, John Wiley & Sons, New York, 2000.
14. F. Ghiam, J. L. Whrre, Phase morphology of injection-molded blends of nylon-6 and polyethylene and comparison with compression molding, *Polymer Engineering Science*, pp. 31-42, 1991.